

# Performance Analysis of a Claw Pole PM Motor Using Improved FEA-Based Phase Variable Model

Youguang Guo<sup>1</sup>, Jianguo Zhu<sup>1</sup>, Jiaxin Chen<sup>2</sup>, Steven Su<sup>1</sup>, Haiyan Lu<sup>1</sup>, and Jianxun Jin<sup>3</sup>

<sup>1</sup>Faculty of Engineering and Information Technology, University of Technology, Sydney, NSW 2007, Australia

<sup>2</sup>College of Electromechanical Engineering, Donghua University, Shanghai, 200051, China

<sup>3</sup>Center of Applied Superconductivity, University of Electronic Science and Technology of China, Chengdu, 610054, China

**Abstract-** This paper presents the performance analysis of a three-phase three-stack permanent magnet (PM) claw pole motor by using an improved phase variable model, which has been developed for accurate and efficient performance simulation of PM brushless dc motors. The improved model can take into account the effect of magnetic saturation and rotor position dependence of key parameters including back electromagnetic force, winding inductance, cogging torque and core loss, which are obtained from time-stepping nonlinear magnetic field finite element analysis (FEA). The presented model has been implemented in Simulink environment and employed to simulate the dynamic and steady-state performance of the three-phase three-stack PM claw pole motor with soft magnetic composite stator. Parameter computation and performance simulation are validated by experiments on the motor prototype.

## I. INTRODUCTION

Thanks to their many advantages such as high power density, high efficiency and high drive performance, permanent magnet (PM) synchronous motors with brushless dc (BLDC) control schemes have been widely applied in industrial and domestic appliances. In the design of a high performance BLDC drive, an accurate and fast model for predicting, evaluating and optimizing the drive system performance is always desirable. Much work has been conducted on the simulation models and performance prediction of BLDC motors by various researchers. However, these analyses are generally based on many assumptions and simplifications such as trapezoidal back electromotive force (EMF), constant winding inductance, constant core loss, and negligible cogging torque. To accurately predict the performance of the BLDC motor, the real waveforms of these parameters against rotor position should be considered [1-3].

For computation of motor parameters and performances, comparing to the equivalent circuit method, magnetic field finite element analysis (FEA) provides more accurate results but can be time consuming. A phase variable model was developed in [3], which can perform much faster than FEA but with the same level of computational accuracy. The rotor dependences of the parameters are previously obtained by a series of FEAs and stored in lookup tables. In BLDC operation, there always exists a phase winding which is non-energized and the voltage of the phase is immeasurable, so the equation-based model cannot be applied to the BLDC motor directly. An alternative model, consisting of several circuit components, has to be used [3].

To overcome the above shortcoming, an improved phase variable model has been introduced, which employs a pure mathematical approach to compute the voltage of the central point of star-connected 3-phase windings so that the voltage of each phase can be obtained and the equation-based model can be directly applied to the BLDC motor [4-5]. The model has been applied to simulate the steady-state and dynamic performance of a 3-phase 3-stack PM claw pole motor with soft magnetic composite (SMC) stator under a sensorless BLDC scheme [6-7], in which the variation of back EMF, winding inductance and cogging torque are considered. This paper presents the performance analysis of the claw pole SMC motor by further including the effect of transient core loss, which usually takes a significant part in the core loss of SMC machines [8]. Both parameter computations and performance simulations are verified by experimental results.

## II. PHASE VARIABLE MODEL

The phase variable model is composed of several electrical and mechanical equations. The voltage equation of phase winding  $j$  ( $j=a, b, c$ ) is given as

$$v_j = r_j i_j + d\lambda_j / dt + e_j \quad (1)$$

where  $v$ ,  $r$ ,  $i$ ,  $\lambda$  and  $e$  are the phase voltage, resistance, current, flux linkage and back EMF, respectively. The flux linkage can be written in terms of apparent inductance as

$$\lambda_j = \sum_{k=a}^c L_{jk} i_k \quad (2)$$

Since the flux linkage is a function of stator currents and rotor position, the second term of (1) can be expanded as

$$\frac{d\lambda_j}{dt} = \sum_{k=a}^c \frac{\partial \lambda_j}{\partial i_k} \frac{di_k}{dt} + \frac{\partial \lambda_j}{\partial \theta_r} \frac{d\theta_r}{dt} = \sum_{k=a}^c (L'_{jk} \frac{di_k}{dt} + \frac{dL_{jk}}{d\theta_r} i_k \omega_r) \quad (3)$$

where  $L_{jk}$  and  $L'_{jk}$  are the apparent and incremental inductances, respectively,  $\theta_r$  is the rotor mechanical angle, and  $\omega_r$  is the rotor angular speed.

Substituting (3) into (1), the voltage equation of the  $j$ -th phase winding becomes

$$v_j = r_j i_j + \sum_{k=a}^c \left( L'_{jk} \frac{di_k}{dt} + \frac{dL_{jk}}{d\theta_r} i_k \omega_r \right) + e_j \quad (4)$$

The electromagnetic torque and motion equation are

$$T_{em} = \left( \sum_{j=a}^c e_j i_j \right) / \omega_r + T_{cog} \quad (5)$$

$$J d\omega_r / dt = T_{em} - P_{fe} / \omega_r - T_L - \delta \omega_r, \quad d\theta_r / dt = \omega_r \quad (6)$$

where  $T_{cog}$  is the cogging torque,  $J$  the total inertia of rotating parts,  $P_{fe}$  the core loss,  $T_L$  the load torque, and  $\delta$  the friction coefficient.

For the symmetrical 3 phase windings, which are star-connected without central line, we have

$$r_j = r_k, \quad L_{jk} = L_{kj}, \quad \sum_{j=a}^c i_j = 0 \quad (j, k=a, b, c) \quad (7)$$

The above equations constitute the so-called phase variable model. The profiles of the back EMF, apparent inductance, incremental inductance, cogging torque and core loss are obtained in advance based on non-linear time-stepping magnetic field FEAs, in which magnetic saturation and rotor position dependence are considered. All these parameters are stored as lookup tables and will be retrieved during the performance simulation according to rotor position or time.

### III. COMPUTATION OF CENTRAL POINT VOLTAGE

Suppose the electrical potentials (voltages) of three phase winding terminals and central point are  $U_a, U_b, U_c$  and  $U_N$ , respectively, we have

$$v_j = U_j - U_N, \quad (j=a, b, c) \quad (8)$$

$$U_N = \sum_{j=a}^c (U_j - v_j) / 3 \quad (9)$$

Substituting (4) into (9) with the consideration of (7), one can obtain:

$$U_N = \frac{1}{3} \sum_{j=a}^c \left[ U_j - \sum_{k=a}^c \left( L'_{jk} \frac{di_k}{dt} + \frac{dL_{jk}}{d\theta_r} i_k \omega_r \right) - e_j \right] \quad (10)$$

The values of  $U_a, U_b$  and  $U_c$  are decided by the switching states of inverter with the 3 phase windings, PWM state, and phase currents. Under the BLDC mode, there are only two phase windings that are excited at each moment, e.g. the current flows into phase  $b$  and then out of phase  $c$  via the

central point, and phase  $a$  is non-energized. Considering (7),  $U_N$  and  $U_a$  can be decided by

$$U_N = \frac{1}{2} \sum_{j=b}^c \left( U_j - L'_{jj} \frac{di_j}{dt} - \frac{dL_{jj}}{d\theta_r} i_j \omega_r - e_j \right) \quad (11)$$

$$U_a = U_N + \sum_{j=a}^c L'_{ja} \frac{di_a}{dt} + e_a + \sum_{k=b}^c \left( L'_{ak} \frac{di_k}{dt} + \frac{dL_{ak}}{d\theta_r} i_k \omega_r \right) \quad (12)$$

When the phase current is not equal to zero and PWM is under the duty-off state,  $U_a$  is decided by

$$U_a = U_{bus} \text{ if } I_a > 0, \quad U_a = 0 \text{ if } I_a < 0 \quad (13)$$

where  $U_{bus}$  is the potential of the power bus line.

Using (11)-(13), one can work out the potentials of the input ports and the central point of the three phase windings, and hence the three phase voltages.

By defining that

$$v_{am} = \sum_{k=b}^c L'_{ak} \frac{di_k}{dt} + \sum_{k=a}^c \frac{dL_{ak}}{d\theta_r} i_k \omega_r \quad (14)$$

and referring to (7), one can obtain

$$v_a = (r_a i_a + L'_{aa} \frac{di_a}{dt}) + v_{am} + e_a \quad (15)$$

$$v'_a = v_a - v_{am} = (r_a i_a + L'_{aa} \frac{di_a}{dt}) + e_a \quad (16)$$

Similarly,  $v_{bm}, v'_b, v_{cm}$  and  $v'_c$  can be defined.

### IV. ANALYSIS OF A PM CLAW POLE SMC MOTOR UNDER BLDC SCHEME BY THE IMPROVED PHASE VARIABLE MODEL

#### A. Implementation of the Improved Phase Variable Model

Based on (1)-(13), a complete simulation model of BLDC is built in Matlab/Simulink environment, as shown in Fig. 1, where  $v_{jm}, v_j$  and  $v'_j$  ( $j=a, b, c$ ) are obtained from a Matlab function according to (14-16). The rest of work is similar to the modeling of a conventional dc motor, so the developed model can be easily realized in Simulink.

By using the model, comprehensive performance of the BLDC motor can be simulated. As an example, the model has been applied to analyze the steady-state and dynamic performance of a 3-phase 3-stack PM claw pole SMC motor, e.g. whether or not the motor can reach the desired speed with the rated load and the rated inverter voltage.

#### B. Motor Prototype

The PM claw pole SMC motor consists of an internal SMC stator (three phases are axially stacked with an angular shift of 120° electrical) and an external mild steel rotor with three

arrays of PMs mounted on the inner surface of the rotor yoke [6-7]. The major dimensions include stator outer diameter of 80 mm, effective axial length of 93 mm, 1 mm main airgap length, and 20 poles. The motor is designed to operate with a sensorless BLDC scheme, delivering a torque of 2.65 Nm at 1800 rpm.

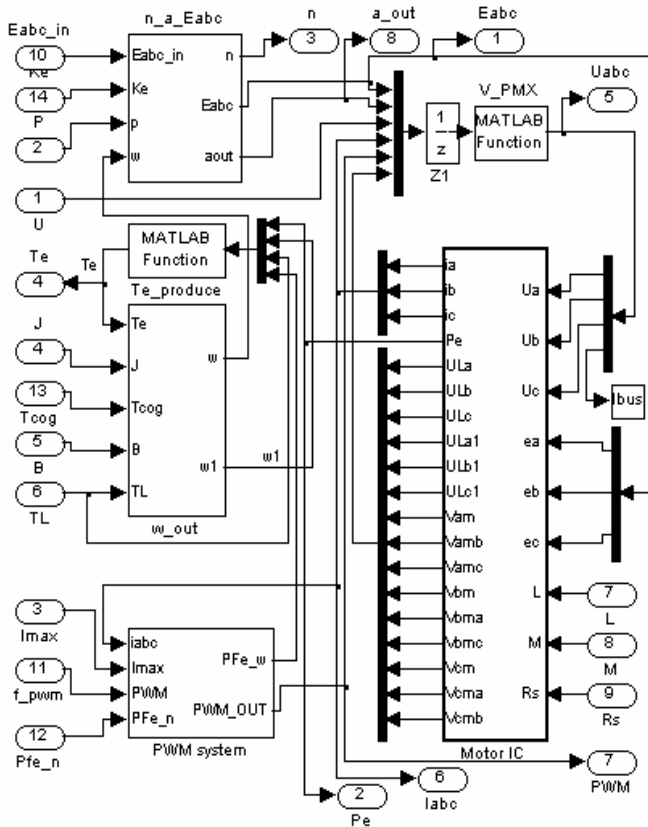


Figure 1. Simulink implementation of the improved BLDC model

### C. Profiles of Key Motor Parameters Determined by FEA

In the developed phase variable BLDC model, the profiles of key motor parameters are previously obtained through nonlinear time-stepping FEA solutions. For example, based on the no-load magnetic field distribution, the waveform of PM flux (defined as the flux of one phase winding produced by rotor PMs) is acquired as in Fig. 2, where the rotor angle  $\theta$  is in electrical degrees,  $\theta = p\theta_r$ ,  $p$  is the number of pole-pairs. It can be seen that the flux waveform is quite sinusoidal. The back EMF can then be inferred by differentiating the PM flux linkage with respect to time (rotor angle). Considering that the PM flux dominates in the total flux of a PM motor, the saturation caused by winding currents is ignored here.

Also from the no-load field solutions, the cogging torque can be obtained by the virtual work or the Maxwell stress tensor methods, as shown in Fig. 3. It can be seen that waveform of the cogging torque is close to a sinusoid with a frequency of 6 times that of the PM flux or back EMF.

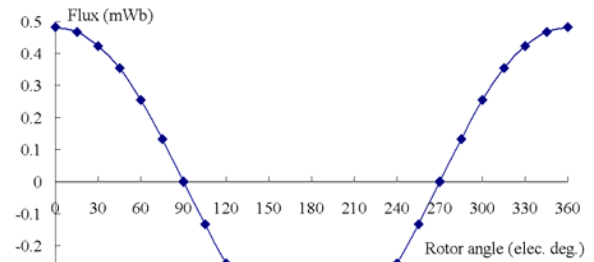


Figure 2. Per-turn flux of one phase winding under no-load

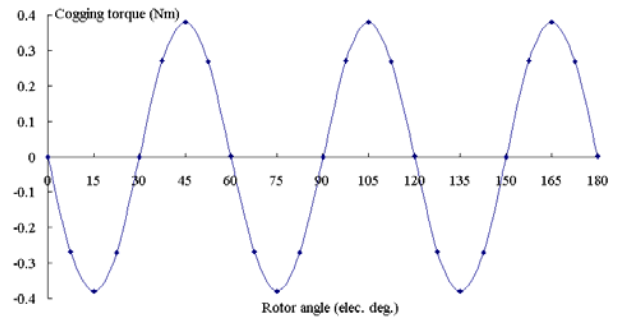


Figure 3. Computed cogging torque of the 3-stack motor

The winding inductances are computed by a modified incremental energy method [9], in which two steps of analyses are conducted. Firstly, a nonlinear analysis with the excitation of rotor PMs is carried out, and both the apparent and incremental permeabilities in each element are stored, which correspond to  $B$  (flux density)/ $H$  (field strength) and  $\Delta B/\Delta H$  at the operating point ( $B$ ,  $H$ ) on the magnetization curve, respectively. Secondly, the remanence of PM is set as zero and a linear analysis is conducted with the saved permeabilities and a current  $i$  in the phase winding to compute the magnetic co-energy  $W'_f$ . It should be noted that the stored apparent permeability should be used for apparent inductance computation and the incremental permeability for incremental inductance. Then, the winding inductance can be computed by

$$L = 2W'_f / i^2 \quad (17)$$

Fig. 4 shows the computed apparent and incremental inductances of one phase winding, as well as the experimental results, which are obtained using the common V-I method by applying a small ac current (0.2 A, 500 Hz).

In a conventional electrical machine, copper loss is the dominant part of total power loss and hence the effect of core loss is not significant and is often considered as a constant. However, in SMC machines, the core loss is comparable to copper loss, so it should be accurately computed and included in the model. The transient core loss of this claw pole motor is computed by the following FEA-based formulations [10]:

$$P_{fe} = \left\{ \sum_{j=x}^z H_j \frac{dB_j}{dt} \right\}^2 \frac{\beta}{2} + \frac{k_c}{2\pi^2} \sum_{j=x}^z \left( \frac{dB_j}{dt} \right)^2 + \frac{k_e}{C_e} \left\{ \sum_{j=x}^z \left( \frac{dB_j}{dt} \right)^2 \right\}^{\frac{3}{4}} \quad (18)$$

where the coefficients  $\beta$ ,  $k_c$ ,  $k_e$  and  $C_e$  are obtained by curve fitting based on the measurements on a cubic SMC sample by using a 3-D magnetic property testing system [11]. The calculation is based on each element, in which the flux density and field strength are obtained by time-stepping FEA.

Fig. 5 shows the curve of core loss against rotor position when the motor runs at 1800 rpm at no-load. The average core loss is about 58 W, which is close to the measurement (61 W) by using the “dummy rotor” method [6].

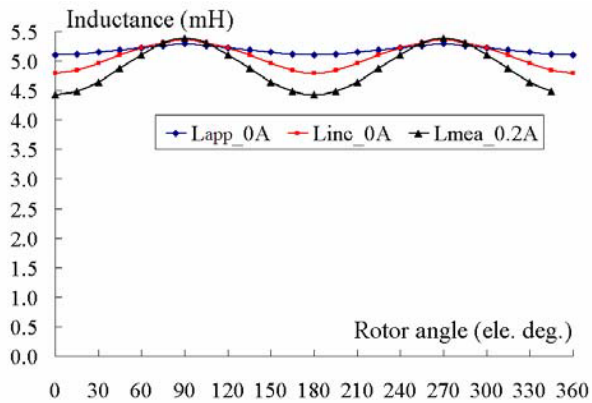


Figure 4. Computed and measured inductance of one phase winding

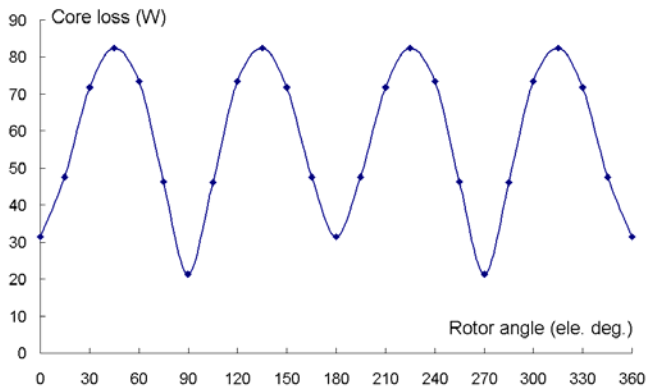


Figure 5. Core loss against rotor angle at 1800 rpm at no-load

#### D. Performance Simulation

Fig. 6 illustrates the simulated curves of speed, electromagnetic torque and power during the start-up with the rated load of 2.65 Nm when the rated inverter dc voltage of 165 V is applied. It can be seen that the motor can accelerate to the rated speed (1800 rpm). As the variations of all major parameters are considered, the simulated speed and torque have more ripples than those results from [6], in which the effect of transient core loss torque was ignored.

More dynamic and steady state performances can be obtained by the presented Simulink-based phase variable

model, e.g. the waveforms of voltage, back EMF and current of phase winding as shown in Fig. 7. The simulations have been validated by the experimental results on the motor prototype [6]. As an example, Fig. 8 plots the measured steady mechanical characteristics. The motor can deliver a torque of 2.65 Nm at 1800 rpm when the inverter dc voltage is 165 V.

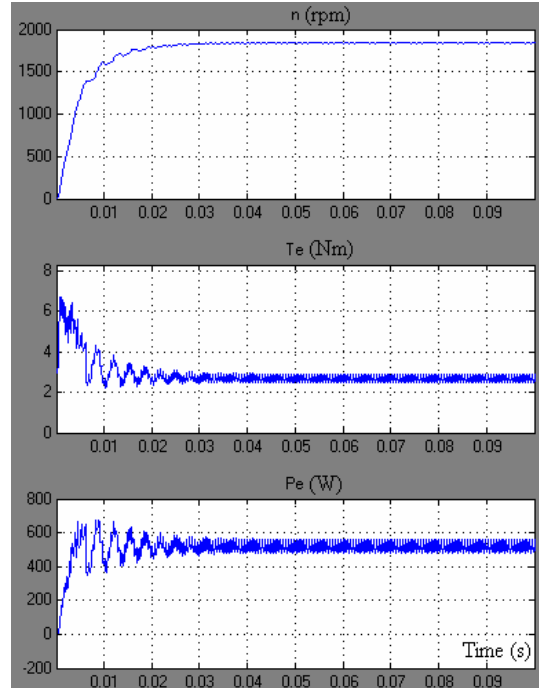


Figure 6. Simulated speed, electromagnetic torque and power during start-up

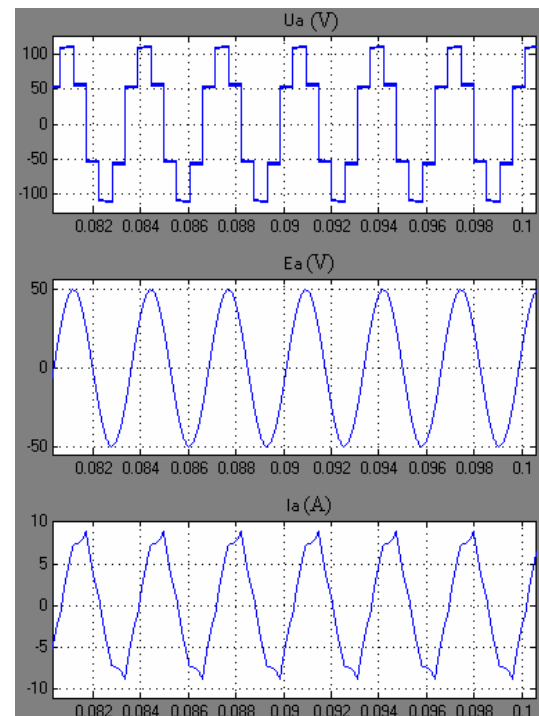


Figure 7. Waveforms of voltage, back EMF and current of a phase winding at steady state

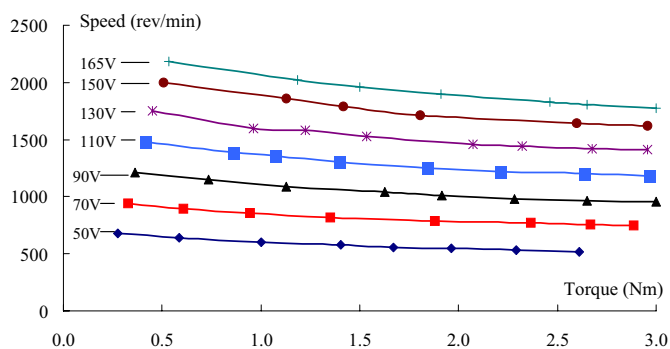


Figure 8. Measured mechanical characteristics

## V. CONCLUSION

This paper presents the performance analysis of a PM claw pole SMC motor under sensorless BLDC control scheme by using an improved phase variable model, in which a mathematical approach is applied to obtain the voltages of both energized and non-energized phases. The effects of variations of all major parameters including back EMF, winding inductance, cogging torque and core loss are considered in the simulation. The calculation of major motor parameters by FEA and the performance simulations are reported and verified by experimental results.

## REFERENCES

- [1] S. L. Ho, W. N. Fu, H. L. Li, H. C. Wong, and H. Tan, "Performance analysis of brushless DC motors including features of the control loop in the finite element modeling," *IEEE Trans. Magn.*, vol. 37, no. 5, pp. 3370-3374, Sep. 2001.
- [2] Y. S. Jeon, H. S. Mok, G. H. Choe, D. K. Kim, and J. S. Ryu, "A new simulation model of BLDC motor with real back EMF waveform," in *Proc. 7th Workshop on Computers in Power Electronics*, Blacksburg, VA, USA, July 2000, pp. 217-220.
- [3] O. A. Mohammed, S. Liu, and Z. Liu, "A phase variable model of brushless DC motors based on finite element analysis and its coupling with external circuits," *IEEE Trans. Magn.*, vol. 41, no. 5, pp. 1576-1579, May 2005.
- [4] J. X. Chen, Y. G. Guo, and J. G. Zhu, "An improved phase variable model based on electro-magnetic field coupled with its external circuits for performance evaluation of permanent magnet brushless dc motors," in *Proc. Int. Conf. on Industrial Electronics and Applications*, Harbin, China, 23-25 May 2007, pp. 955-959.
- [5] J. X. Chen, Y. G. Guo, J. G. Zhu, and J. X. Jin, "Performance analysis of a surface mounted permanent magnet brushless dc motor using an improved phase variable model," in *Proc. 42<sup>nd</sup> IEEE Industry Applications Society Annual Conference*, New Orleans, USA, 23-27 Sept. 2007, pp. 2169-2174.
- [6] Y. G. Guo, J. X. Chen, J. G. Zhu, H. W. Lu, H. Y. Lu, and J. X. Jin, "An improved phase variable model for dynamic performance analysis of a PM claw pole SMC motor with brushless dc control," in *Proc. Australasian Universities Power Engineering Conference*, Melbourne, Australia, 10-13 Dec. 2006, paper TS1-02.
- [7] Y. G. Guo, J. G. Zhu, Z. W. Lin, H. Y. Lu, X. L. Wang, and J. X. Chen, "Influence of inductance variation on the performance of a PM claw pole SMC motor," *Journal of Applied Physics*, vol. 103, no. 7, pp. 07F118-1-3, 1 Apr. 2008.
- [8] Y. G. Guo and J. G. Zhu, "Application of soft magnetic composite materials in electrical machines, a review," *Australian Journal of Electrical & Electronics Engineering*, vol. 3, no. 1, pp. 37-46, 2006.
- [9] Y. G. Guo, J. G. Zhu, and H. Y. Lu, "Accurate determination of parameters of a claw pole motor with SMC stator core by finite element magnetic field analysis," *IEE Proc. - Electri. Power Appl.*, vol. 153, no. 4, pp. 568-574, July 2006.
- [10] D. Lin, P. Zhou, W. N. Fu, Z. Badics, and Z. J. Cendes, "A dynamic core loss model for soft ferromagnetic and power ferrite materials in transient finite element analysis," *IEEE Trans. Magn.*, vol. 40, no. 2, pp. 1318-1321, Mar. 2004.
- [11] Y. G. Guo, J. G. Zhu, Z. W. Lin, and J. J. Zhong, "Measurement and modeling of core losses of soft magnetic composites under 3D magnetic excitations in rotating motors," *IEEE Trans. Magn.*, vol. 41, no. 10, pp. 3925-3927, Oct. 2005.